Journal of Alloys and Compounds 516 (2012) 27–32

Contents lists available at SciVerse ScienceDirect

Journal of Alloys and Compounds

journal homepage: www.elsevier.com/locate/jallcom

Synthesis of metal aluminate nanoparticles by sol–gel method and studies on their reactivity

Nisha Bayal, P. Jeevanandam*

Department of Chemistry, Indian Institute of Technology Roorkee, Roorkee 247667, India

ARTICLE INFO

Article history:
Received 1 September 2011
Received in revised form
11 November 2011
Accepted 20 November 2011
Available online 9 December 2011

Keywords:
Oxide nanoparticles
Metal aluminate
Sol–gel method
Reactivity

ABSTRACT

Nanosized metal aluminates ($CoAl_2O_4$, $NiAl_2O_4$ and $CuAl_2O_4$) were prepared by sol–gel method. The formation of metal aluminate nanoparticles and their particle size were found to depend upon the calcination temperature. $CoAl_2O_4$ nanoparticles were obtained at 700 °C, which is much lower than that required for its preparation through solid state reactions. The formation of $NiAl_2O_4$ and $CuAl_2O_4$ nanoparticles occurs at 900 °C and 800 °C, respectively. Characterization of the metal aluminate nanoparticles were carried out by X-ray diffraction, thermal gravimetric analysis, UV–vis diffuse reflectance spectroscopy, FT-IR spectroscopy, scanning electron microscopy and transmission electron microscopy. The chemical reactivity of the synthesized metal aluminate nanoparticles were also tested using paraoxon destructive adsorption and catalytic reduction of 4-nitro phenol.

1. Introduction

Nanocrystalline metal aluminates possess important applications in various fields such as heterogeneous catalysis, pigments, sensors and ceramics [1–6]. Aluminate spinels have been used as catalysts in the decomposition of methane, steam reforming, dehydration of saturated alcohols to olefins, dehydrogenation of alcohols, etc. [7–11]. Aluminate nanoparticles have also been reported as good photocatalysts, e.g. for the degradation of methyl orange [12].

The general formula of spinels is AB_2O_4. In the spinel structure, the anions are arranged in a cubic close packed array with the cations arranged in the holes of the array. There are eight tetrahedral and four octahedral holes per molecule. In the case of normal spinels, the A^{2+} ions occupy tetrahedral holes and B^{3+} ions are present in the octahedral holes. In the case of inverse spinels, one half of A^{2+} ions occupy tetrahedral holes and the remainder of A^{2+} ions and all B^{3+} ions occupy the octahedral holes [13]. It is known that the nature of occupancy of tetrahedral and octahedral sites depends on the calcination temperature [14].

Metal aluminate nanocrystalline powders are generally prepared using solid state high temperature reactions. The temperature is usually greater than 1000 °C which influences the particle size [15,16]. One of the disadvantages of the high temperature method is that the product obtained usually possesses low surface area. Solution based methods that have been reported for the preparation of metal aluminate nanoparticles include co-precipitation, polymeric precursor method, combustion and sol–gel method [17–20]. The preparation of spinels by co-precipitation often leads to non-uniform materials since it is difficult to precipitate, homogenously, materials in large batches. Metal aluminate nanoparticles have been prepared by other methods such as solvothermal synthesis [21,22], supercritical method [23], spray pyrolysis [24], flame synthesis [25], thermolysis [26], chemical vapour deposition [27] and sonochemical synthesis [28].

Sol–gel method has been a good option to produce homogenous materials since in this method, the chemical elements become uniformly distributed during the gel formation step [17]. Sol–gel method also offers good stoichiometric control and production of ultrafine particles with narrow size distribution at comparatively low temperatures [29,30]. Sol–gel method has been used to prepare the metal aluminate nanoparticles by different authors. For example, Stranger and Orel have reported the synthesis of $CoAl_2O_4$ nanoparticles using ethylacetoacetate as the chelating agent [31]. Cui et al. have reported the preparation of $NiAl_2O_4$ nanoparticles using propylene oxide as the gelation agent [32]. The synthesis of nickel, copper and cobalt aluminate nanoparticles using single source heterobimetallic alkoxides as precursors is also known in the literature [30]. In the present study, metal aluminate nanoparticles such as $CoAl_2O_4$, $NiAl_2O_4$ and $CuAl_2O_4$ have been synthesized without using any chelating/gelating agent. Two different metal

* Corresponding author. Tel.: +91 1332 285444; fax: +91 1332 286202.
E-mail address: jeevafcy@iitr.ernet.in (P. Jeevanandam).

0925-8388/$ – see front matter © 2011 Elsevier B.V. All rights reserved.
doi:10.1016/j.jallcom.2011.11.080

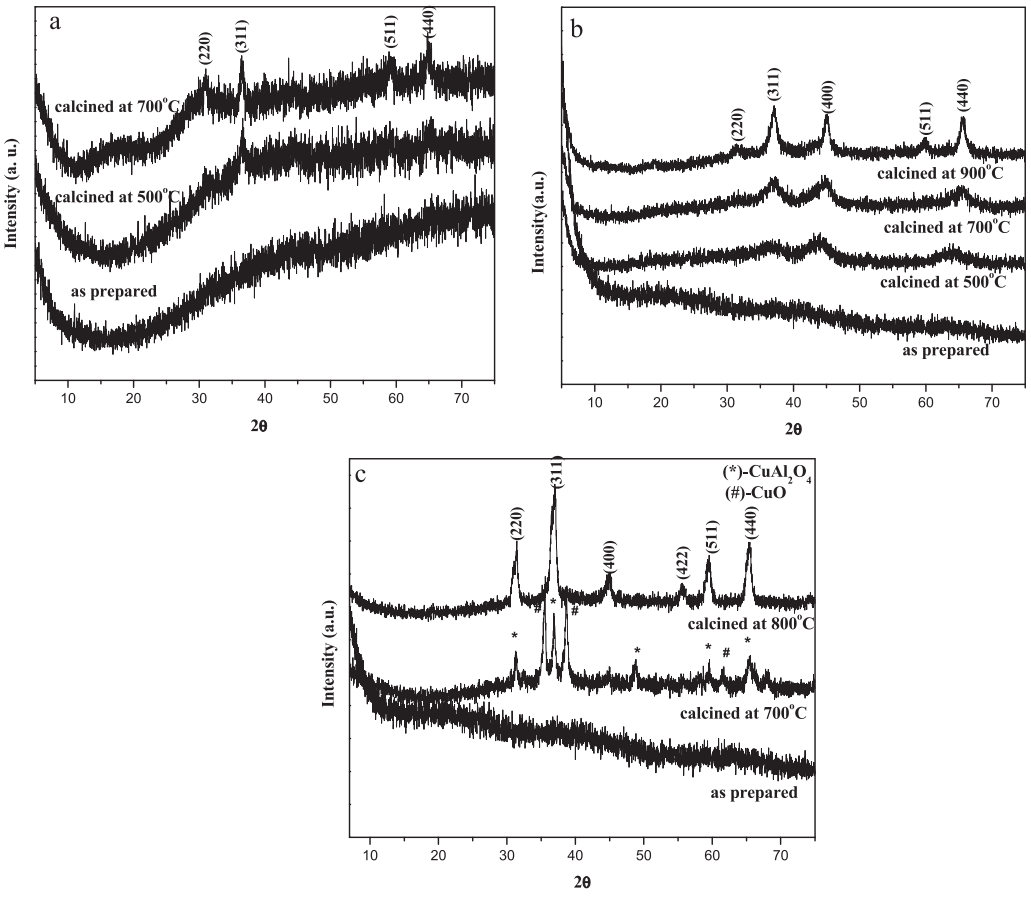

Fig. 1. XRD patterns of metal aluminate nanoparticles: (a) $CoAl_2O_4$, (b) $NiAl_2O_4$ and (c) $CuAl_2O_4$.

precursors were used instead of bimetallic alkoxide precursors during the sol–gel process.

2. Experimental

In the present study, MAl_2O_4 (M = Co, Ni, Cu) nanoparticles were synthesized using suitable precursors by the sol–gel method. The as prepared precursors were subjected to calcination in the temperature range 500–900 °C to obtain the nanocrystalline spinels.

The chemicals used for synthesis of the spinels were aluminum isopropoxide (Aldrich), cobalt acetylacetonate (Alfa Aesar), nickel acetate (Aldrich), cupric acetate (RANKEM), ethanol, toluene and Millipore water. All the chemicals were used as received. More details on the synthesis of MAl_2O_4 nanoparticles are as follows.

Metal precursors (Co-aceylacetonate, Ni-acetate, and Cu-acetate for $CoAl_2O_4$, $NiAl_2O_4$ and $CuAl_2O_4$, respectively) and Al-isopropoxide were taken in a 1:2 molar ratio and placed in a round bottom flask. Then, a mixture of 100 ml toluene and 40 ml ethanol were added and the suspension was stirred vigorously to prepare a homogenous mixture. Afterwards, about 1.0 ml of distilled water was added drop wise with continuous stirring. The mixture was stirred overnight at room temperature (25 °C). The sol obtained was then evaporated at 80 °C to get a gel. The gel was dried for a few hours at 80 °C inside a drying cabinet and then grounded to obtain the xerogel powder. The as prepared powders were subjected to heat treatment in air at 500–900 °C (heating rate = 2 °C/min).

X-ray powder diffraction patterns were recorded using a Bruker AXS-D8 diffractometer (Cu Kα radiation) with a step size of $2\theta = 0.02°$. FT-IR spectra were recorded with a NEXUS Thermo Nicolet IR-spectrometer using KBr pellets. The range studied was 4000–400 cm^{-1}. Diffuse reflectance spectra were recorded with the help of a Shimadzu UV-3600 UV-Vis NIR spectrometer attached with a diffuse reflectance accessory. $BaSO_4$ was used as the reference. Field emission-SEM images of the aluminate nanoparticles were obtained with the help of FEI Quanta 200F electron microscope operating at an accelerating voltage of 20 kV. TEM measurements were performed on a JEOL model 1200EX instrument operated at an accelerating voltage of 120 kV. The powder samples were dispersed in isopropanol using low power sonication before putting a drop over carbon coated copper grid followed by drying for the measurements.

3. Results and discussions

The powder XRD patterns of as prepared and calcined cobalt aluminate samples are shown in Fig. 1a. The as prepared sample is X-ray amorphous. It can be noted that the sample calcined at 500 °C is less crystalline compared to that calcined at 700 °C. The observed '*d*' values of the sample calcined at 700 °C was found to match with that of $CoAl_2O_4$ (JCPDS file no. 82-2252). It should be noted that the XRD pattern of Co_3O_4 is close to that of $CoAl_2O_4$, however, with a minor difference [33]. The crystallite size of $CoAl_2O_4$, calculated using Debye Scherrer formula, is about 13.7 nm. The XRD patterns of nickel aluminate samples calcined at 700–900 °C along with that of the as prepared are shown in Fig. 1b. The samples calcined at 700 °C as well as at 800 °C were of light-green color. After calcination at 900 °C, a light blue colored compound characteristic of $NiAl_2O_4$ was obtained [32]. The XRD pattern of the sample calcined at 900 °C clearly shows the spinel structure (JCPDS file no. 10-0339). The calculated crystallite size of $NiAl_2O_4$ is about 8.7 nm. The X-ray diffraction patterns of products corresponding to the $CuAl_2O_4$ synthesis (Fig. 1c) indicate that the sample calcined at 700 °C consists of two phases; $CuAl_2O_4$ (JCPDS file no. 78-1605) and CuO (JCPDS file no. 78-0428). The XRD peaks due to CuO disappear on calcination at 800 °C and the XRD pattern shows the formation of monophasic copper aluminate nanoparticles with a crystallite size of 9.7 nm.

The thermal gravimetric analysis patterns for as prepared powder samples corresponding to all the three aluminates show three steps weight loss (Fig. 2). The first two weight loss steps in the temperature range 25–200 °C correspond to the loss of adsorbed water molecules [34]. The third weight loss step at about 300 °C and 326 °C in case of $CoAl_2O_4$ and $NiAl_2O_4$ precursors, respectively

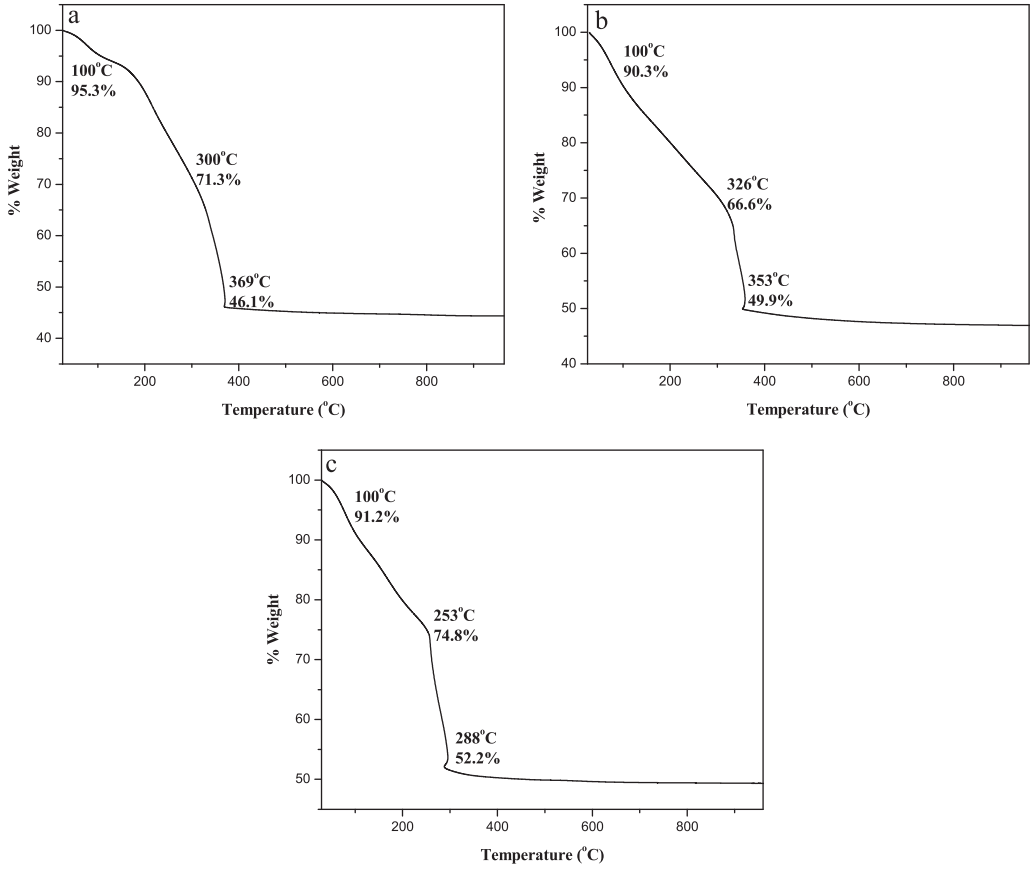

Fig. 2. Thermal gravimetric analysis patterns of metal aluminate precursors: (a) $CoAl_2O_4$, (b) $NiAl_2O_4$ and (c) $CuAl_2O_4$.

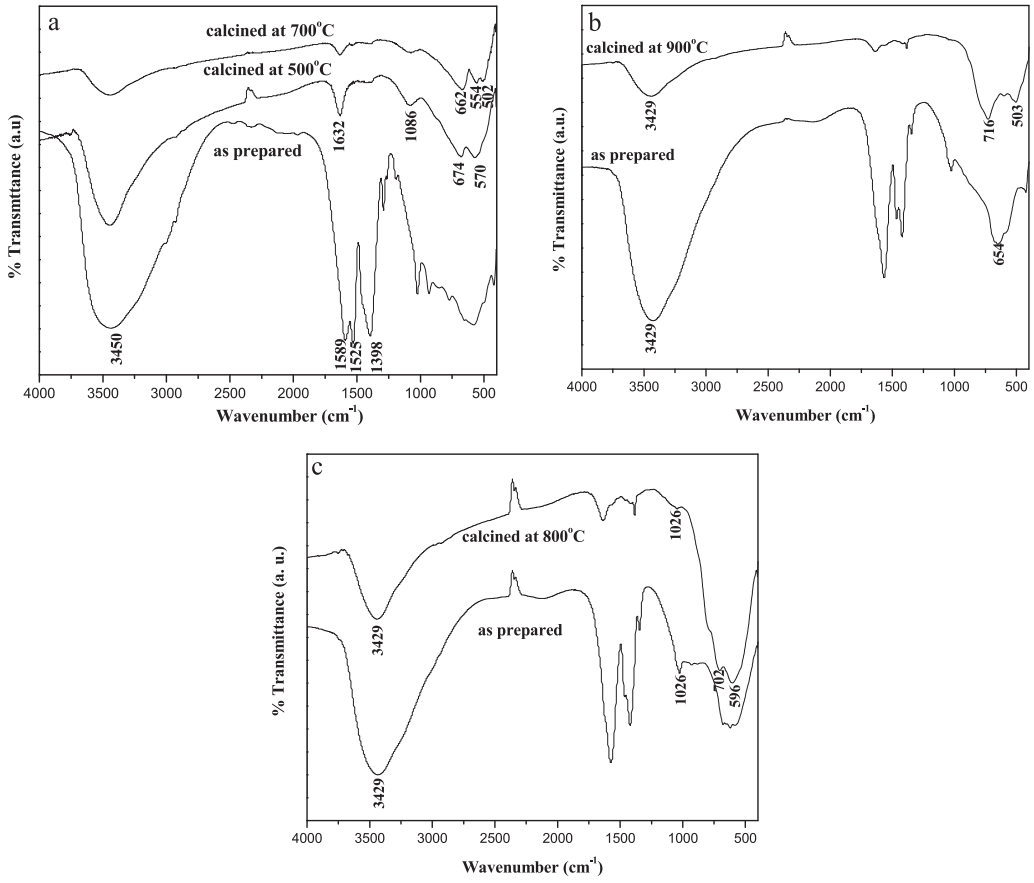

Fig. 3. FT-IR spectra of metal aluminate nanoparticles: (a) $CoAl_2O_4$, (b) $NiAl_2O_4$ and (c) $CuAl_2O_4$.

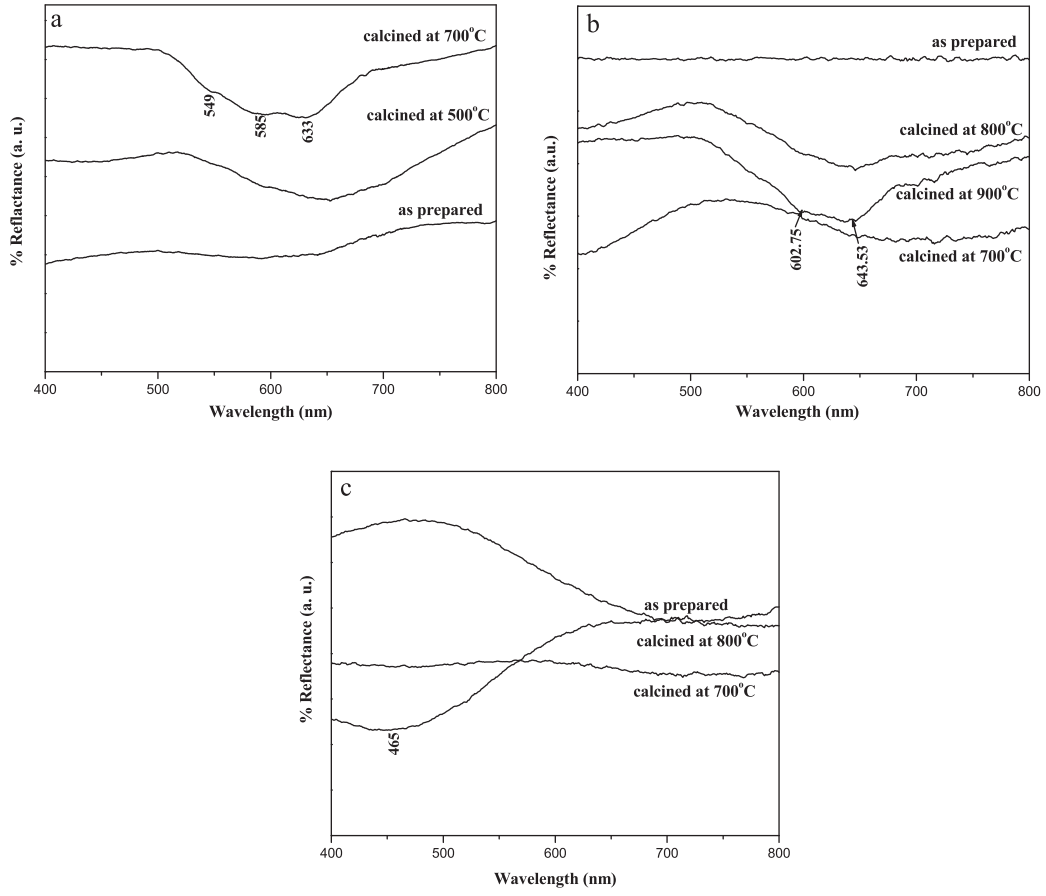

Fig. 4. Diffuse reflectance spectra of metal aluminate nanoparticles: (a) $CoAl_2O_4$, (b) $NiAl_2O_4$ and (c) $CuAl_2O_4$.

and at 253 °C, in the case of $CuAl_2O_4$ precursor, is attributed to decarboxylation and condensation of $Al(OH)_3$ [35].

The FT-IR spectra of as prepared and calcined aluminate samples show broad bands at about 3430 cm^{-1} which can be attributed to hydroxyl stretching (Fig. 3). The band at 1635 cm^{-1} is assigned to the bending vibrational mode of water molecules. There is no IR band present in the region 1028–1157 cm^{-1} in all the three aluminate samples which confirms the absence of Al—OH bending mode [36]. In all the three spinels, the metal-oxygen stretching frequencies are reported in the range 500–900 cm^{-1}, associated with the vibrations of M—O, Al—O and M—O—Al bonds [5]. The FT-IR spectrum of $CoAl_2O_4$ precursor calcined at 500 °C exhibits two broad bands at about 570 and 674 cm^{-1} (Fig. 3a) and these bands are assigned to Co_3O_4. On heating the sample at 700 °C, new bands appear around 502, 554 and 662 cm^{-1} that can be attributed to the vibrational bands of $CoAl_2O_4$ [31]. The Ni—O stretching is observed at about 503 cm^{-1} in the IR spectrum of $NiAl_2O_4$ (Fig. 3b). In the IR spectrum of $CuAl_2O_4$ sample calcined at 800 °C (Fig. 3c), two IR bands appear at about 596 and 702 cm^{-1} which indicate that the product is spinel [37].

Fig. 4 shows the diffuse reflectance spectra of metal aluminate nanoparticles calcined at different temperatures. The color of the metal aluminates is due to d–d transitions. $CoAl_2O_4$ is a normal spinel in which Co^{2+} is tetrahedrally coordinated. Thus, three electronic transitions are spin allowed ($^4A_2$ (F) → $^4T_1$ (P)) where as another three are spin forbidden ($^4A_2$ (F) → $^2T_1$ (G)) [37]. The UV–visible spectrum of as prepared precursor to $CoAl_2O_4$ exhibits no characteristic absorption bands. The sample calcined at 700 °C shows bands at about 549, 585 and 633 nm and these three bands are attributed to $^4A_2$ (F) → $^4T_1$ (P) transitions [38,39]. $NiAl_2O_4$ is an inverse spinel. The DRS spectrum of $NiAl_2O_4$ calcined at 900 °C (Fig. 4b) shows two bands at about 603 nm and 644 nm. These bands are attributed to Ni^{2+} in octahedral sites and tetrahedral sites, respectively [40,41]. The diffuse reflectance spectrum of $CuAl_2O_4$ sample calcined at 800 °C (Fig. 4c) has a broad adsorption band at about 465 nm which can be assigned to $CuAl_2O_4$ spinel [42].

The FE-SEM images of the aluminate nanoparticles showed irregular morphology of nanoparticles with agglomeration. The EDX analysis data for $CoAl_2O_4$ calcined at 700 °C and $NiAl_2O_4$ sample calcined at 900 °C indicated the expected atomic ratio of elements (*i.e.* at.% of Co to Al = 1:2 and Ni to Al = 1:2). The atomic ratio of Cu to Al in the case of $CuAl_2O_4$ nanoparticles (calcination temperature = 800 °C) was 1:2.8, and it is proposed that the product is a mixture of $CuAl_2O_4$ and amorphous Al_2O_3. The TEM images of the aluminate nanoparticles are shown in Fig. 5. It can be noticed that the aluminate nanoparticles are agglomerated. The average particle size for $CoAl_2O_4$, $NiAl_2O_4$ and $CuAl_2O_4$ nanoparticles, as calculated from the TEM images, were 9.4 nm, 6.3 nm and 24.1 nm, respectively.

The catalytic activity of the synthesized metal aluminate nanoparticles was tested using reduction of aqueous 4-nitrophenol by sodium borohydride. This reaction has been used for testing the catalytic activity of metal oxide nanoparticles by many authors [1,43,44]. An aqueous solution of 4-nitrophenol is yellow colored and this is due to the presence of nitrophenolate ions. These ions on reduction with $NaBH_4$ form 4-aminophenolate ions which are colorless. The rate of this catalytic reduction depends on the concentration of reagents, temperature and surface area of the catalyst. It is well known, for the reactions involving nanocatalysts, rate of the reaction also depends on the size and shape of the nanoparticles [44].

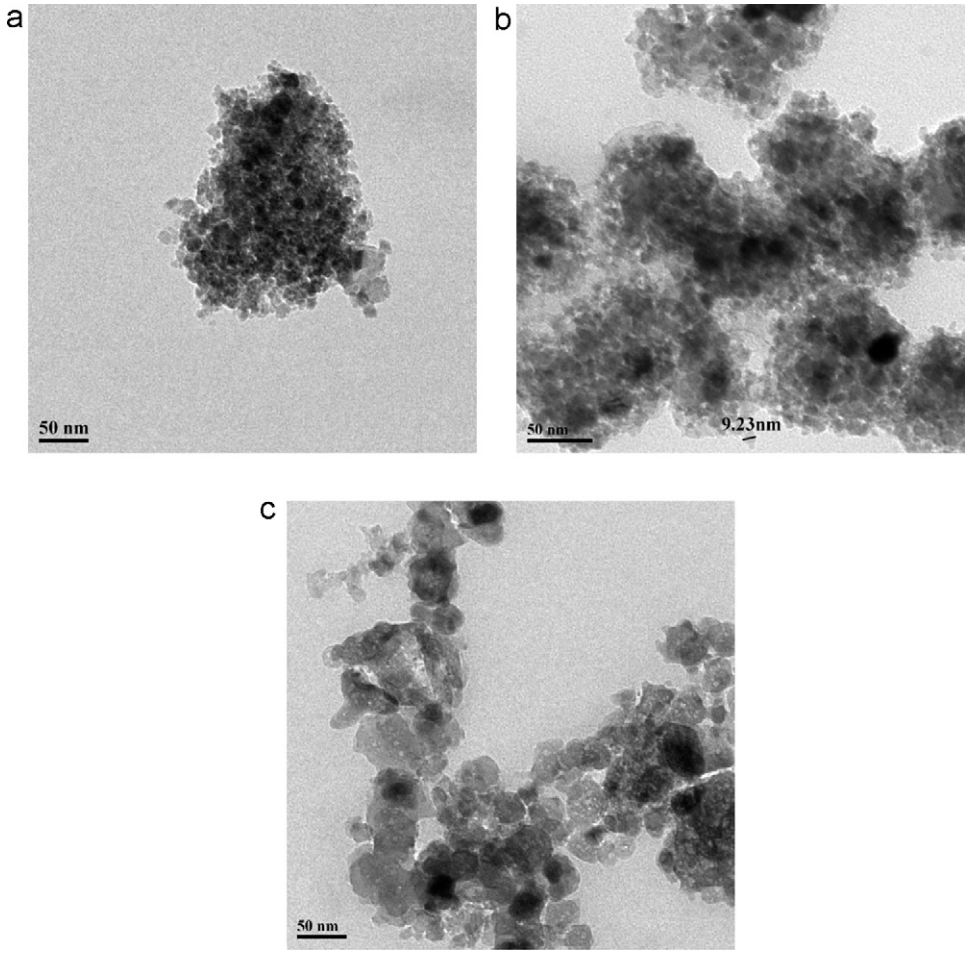

Fig. 5. TEM micrographs of (a) $CoAl_2O_4$ nanoparticles after calcination at 700 °C, (b) $NiAl_2O_4$ nanoparticles after calcination at 900 °C and (c) $CuAl_2O_4$ nanoparticles after calcination at 800 °C.

For the catalytic activity test of the synthesized aluminate nanoparticles [1], four 250 ml beakers were taken. In each beaker, 50 ml aqueous solution of 4-nitrophenol (0.1 mmol) was added and 50 ml of freshly prepared aqueous solution of $NaBH_4$ (0.529 mol/L) was added. Then, about 1×10^{-4} M of the catalyst (metal aluminate nanoparticles) was introduced into the mixture. The mixtures were stirred at room temperature. A blank reaction was also carried out without the catalyst. The time required for the decolorization of yellow color for each set was noted (Table 1). It can be observed from Table 1 that $CuAl_2O_4$ nanoparticles decolorize 4-nitrophenol quickly (2 min) indicating the highest catalytic activity compared to $NiAl_2O_4$ and $CoAl_2O_4$ nanoparticles. According to the reported mechanism [45], the borohydride ions absorb on the surface of the metal aluminate nanoparticles and transfer a surface hydrogen species to the surface. The nitrophenolate ions are adsorbed on the surface of the nanoparticles and then reduced to aminophenolate ions which are desorbed afterwards.

Table 1
Time required for the complete decolorization of yellow color of 4-nitrophenol in the presence of different metal aluminate nanoparticles as catalysts.

Sl. no.	Reaction condition	Time required for decolorization (min)
1.	4-Nitrophenol + $NaBH_4$ (no catalyst)	97
2.	4-Nitrophenol + $NaBH_4$ + $CuAl_2O_4$ nanoparticles	2
3.	4-Nitrophenol + $NaBH_4$ + $NiAl_2O_4$ nanoparticles	14
4.	4-Nitrophenol + $NaBH_4$ + $CoAl_2O_4$ nanoparticles	47

Paraoxon (diethyl 4-nitrophenyl phosphate) is an organophosphate and has been used to test the chemical reactivity of nanocrystalline metal oxides via destructive absorption [46,47]. In the present study, the reactivity of different synthesized metal aluminate nanoparticles were tested using paraoxon. Paraoxon shows

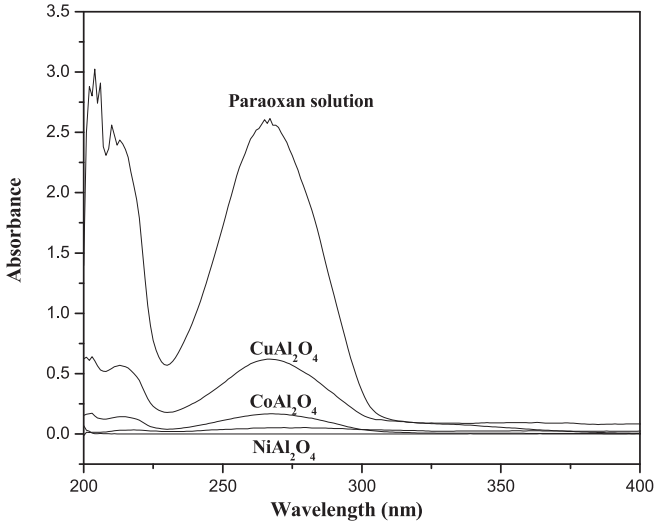

Fig. 6. UV–vis spectra for monitoring the destructive adsorption of paraoxon on different aluminate nanoparticles.

a characteristic UV–visible absorption band at about 265 nm and by following this absorption band, the reactivity of the metal aluminate nanoparticles can be monitored. For testing the chemical reactivity of synthesized aluminate nanoparticles with paraoxon, a solution of 5 μl paraoxon in 100 ml pentane was prepared. Three sets of 100 ml round bottom flasks were taken. Then, 25 ml of the paraoxon solution was taken in each flask and 50 mg each of the aluminate nanoparticles were introduced. The mixtures were stirred for 3 h at room temperature and then UV–vis spectra were recorded (Fig. 6). The UV–vis spectral results indicate that $NiAl_2O_4$ nanoparticles show better destructive adsorption compared to the $CoAl_2O_4$ and $CuAl_2O_4$ nanopaticles.

4. Conclusions

MAl_2O_4 nanoparticles (M = Co, Ni, Cu) were synthesized by a simple sol–gel method without using any gelating agent. The nanoparticles were characterized using an array of techniques. It was found that the calcination temperature affects the formation of nanopartices. The method used here may be extended for the synthesis of other spinel nanoparticles. On the basis of the catalytic activity test using 4-nitrophenol decolorization, it has been found that $CuAl_2O_4$ nanoparticles possess better catalytic activity compared to $CoAl_2O_4$ and $NiAl_2O_4$ nanoparticles. In the destructive adsorption reaction of paraoxon, the performance of $NiAl_2O_4$ is better than that of $CoAl_2O_4$ and $CuAl_2O_4$ nanoparticles.

Acknowledgement

The award of junior research fellowship (JRF) to Ms. Nisha Bayal by the Council of Scientific and Industrial Research, Government of India is gratefully acknowledged.

References

[1] D. Dhak, P. Pramanik, J. Am. Ceram. Soc. 89 (2006) 1014.
[2] C. Feldmann, Adv. Mater. 13 (2001) 1301.
[3] C.R. Michel, Sens. Actuators B 147 (2010) 635.
[4] C.R. Michel, J. Rivera, A.H. Martinez, M.S. Aranda, J. Electrochem. Soc. 155 (2008) 263.
[5] P.M.T. Cavalcante, M. Dondi, G. Guarini, M. Raimondo, G. Baldi, Dyes Pigments 80 (2009) 226.
[6] G. Busca, V. Lorenzelli, V.S. Escribano, R. Guidetti, J. Catal. 131 (1991) 167.
[7] L. Dussault, J.C. Dupin, C. Guimon, M. Monthioux, N. Latorre, T. Ubieto, E. Romeo, C. Royo, A. Monzon, J. Catal. 251 (2007) 223.
[8] N. Salhi, A. Boulahouache, C. Petit, A. Kiennemann, C. Rabia, Int. J. Hydrogen Energy 36 (2011) 11433.
[9] L. Nakka, J.E. Molinari, I.E. Wachs, J. Am. Chem. Soc. 131 (2009) 15544.
[10] Y. Cesteros, P. Salagre, F. Medina, J.E. Sueiras, Appl. Catal. B: Environ. 25 (2000) 213.
[11] N.F.P. Ribeiro, R.C.R. Neto, S.F. Moya, M.M.V.M. Souza, M. Schmal, Int. J. Hydrogen Energy 35 (2010) 11725.
[12] W. Lv, B. Liu, Q. Qiu, F. Wang, Z. Luo, P. Zhang, S. Wei, J. Alloys Compd. 479 (2009) 480.
[13] V. Sepelak, I. Bergmann, S. Indris, A. Feldhoff, H. Hahn, K.D. Becker, C.P. Grey, P. Heitjans, J. Mater. Chem. 21 (2011) 8332.
[14] M. Lo Jacono, M. Schiavello, A. Cimino, J. Phys. Chem. 75 (1971) 1044.
[15] D. Mazza, A. Delmastro, S. Ronchetti, J. Eur. Ceram. Soc. 20 (2000) 699.
[16] P.H. Bolt, F.H.P.M. Habraken, J.W. Geus, J. Solid State Chem. 135 (1998) 59.
[17] D. Segal, J. Mater. Chem. 7 (1997) 1297.
[18] S. Chokkaram, R. Srinivasan, D.R. Milburn, B.H. Davis, J. Mol. Catal. 121 (1997) 157.
[19] L. Gama, M.A. Ribeiro, B.S. Barros, R.H.A. Kiminami, I.T. Weber, A.C.F.M. Costa, J. Alloys Compd. 483 (2009) 453.
[20] W. Li, J. Li, J. Guo, J. Eur. Ceram. Soc. 23 (2003) 2289.
[21] W. Staszak, M. Zawadzki, J. Okal, J. Alloys Compd. 492 (2009) 500.
[22] M. Zawadzki, J. Alloys Compd. 439 (2007) 312.
[23] D. Rangappa, S. Ohara, T. Naka, A. Kondo, M. Ishii, T. Adschiri, J. Mater. Chem. 17 (2007) 4426.
[24] C. Li, Y. Imai, Y. Adachi, H. Yamada, K. Nishikubo, C.N. Xu, J. Am. Ceram. Soc. 90 (2007) 2273.
[25] T. Johannessen, J.R. Jensen, M. Mosleh, J. Johansen, U. Quaade, H. Livbjerg, Chem. Eng. Res. Des. 82 (2004) 1444.
[26] C. Koh, S. Tahir, A. Sen, A. Pathak, P. Pramanik, Br. Ceram. Trans. 101 (2002) 114.
[27] M. Veith, Mater. Sci. Forum 343–346 (2000) 531.
[28] W. Lv, Z. Luo, H. Yang, B. Liu, W. Weng, J. Liu, Ultrason. Sonochem. 17 (2010) 344.
[29] F. Davar, M.S. Niasari, J. Alloys Compd. 509 (2011) 2487.
[30] F. Meyer, R. Hempelmann, S. Mathur, M. Veith, J. Mater. Chem. 9 (1999) 1755.
[31] U.L. Stangar, B. Orel, M. Krajnc, J. Sol–Gel Sci. Technol. 26 (2003) 771.
[32] H. Cui, M. Zayat, D. Levy, J. Non-Cryst. Solids 351 (2005) 2102.
[33] L. Ji, J. Lin, H.C. Zeng, Chem. Mater. 12 (2000) 3466.
[34] W. Schmidt, C. Weidenthaler, Microporous Mesoporous Mater. 48 (2001) 89.
[35] A.V. Ghule, K. Ghule, S.H. Tzing, T.H. Punde, H. Chang, Y.C. Ling, J. Solid State Chem. 182 (2009) 3406.
[36] Z. Zhong, Y. Mastai, Y. Kotypin, Y. Zhao, A. Gedenken, Chem. Mater. 11 (1999) 2350.
[37] M.S. Niasari, F. Davar, M. Farhadi, J. Sol–Gel Sci. Technol. 51 (2009) 48.
[38] D.M.A. Melo, J.D. Cunha, J.D.G. Fernandes, M.I. Bernardi, M.A.F. Melo, A.E. Martinelli, Mater. Res. Bull. 38 (2003) 1559.
[39] D. Rangappa, T. Naka, A. Kondo, M. Ishii, T. Adschiri, J. Am. Chem. soc. 129 (2007) 11061.
[40] P. Jeevanandam, Y. Koltypin, A. Gedanken, Mater. Sci. Eng. B 90 (2002) 125.
[41] M.M. Amini, L. Torkian, Mater. Lett. 57 (2002) 639.
[42] T. James, M. Padmanabhan, K.G.K. Warrier, S. Sugunan, Mater. Chem. Phys. 103 (2007) 248.
[43] Y.C. Chang, D.H. Chen, J. Hazard. Mater. 165 (2009) 664.
[44] M.A. Mahmoud, F. Saira, M.A. El Sayed, Nano Lett. 10 (2010) 3764.
[45] S. Wunder, F. Polzer, Y. Lu, Y. Mei, M. Ballauff, J. Phys. Chem. C 114 (2010) 8814.
[46] P. Jeevanandam, K.J. Klabunde, Langmuir 19 (2003) 5491.
[47] G.M. Medine, V. Zaikovski, K.J. Klabunde, J. Mater. Chem. 14 (2004) 757–763.